Altered Membrane Dynamics of Quantum Dot-Conjugated Integrins during Osteogenic Differentiation of Human Bone Marrow Derived Progenitor Cells

Hongfeng Chen,* Igor Titushkin,* Michael Stroscio,† and Michael Cho*
*Department of Bioengineering and †Department of Electrical and Computer Engineering, University of Illinois, Chicago, Illinois 60607

ABSTRACT Functionalized quantum dots offer several advantages for tracking the motion of individual molecules on the cell surface, including selective binding, precise optical identification of cell surface molecules, and detailed examination of the molecular motion without photobleaching. We have used quantum dots conjugated with integrin antibodies and performed studies to quantitatively demonstrate changes in the integrin dynamics during osteogenic differentiation of human bone marrow derived progenitor cells (BMPCs). Consistent with the unusually strong BMPC adhesion previously observed, integrins on the surface of undifferentiated BMPC were found in clusters and the lateral diffusion was slow (e.g., $\sim 10^{-11}$ cm^2/s). At times as early as those after a 3-day incubation in the osteogenic differentiation media, the integrin diffusion coefficients increased by an order of magnitude, and the integrin dynamics became indistinguishable from that measured on the surface of terminally differentiated human osteoblasts. Furthermore, microfilaments in BMPCs consisted of atypically thick bundles of stress fibers that were responsible for restricting the integrin lateral mobility. Studies using laser optical tweezers showed that, unlike fully differentiated osteoblasts, the BMPC cytoskeleton is weakly associated with its cell membrane. Based on these findings, it appears likely that the altered integrin dynamics is correlated with BMPC differentiation and that the integrin lateral mobility is restricted by direct links to microfilaments.

INTRODUCTION

Regulation of bone marrow derived progenitor cell (BMPC) differentiation offers exciting possibilities for numerous biomedical and clinical applications. There are now focused research efforts directed at the manipulation and control of cell differentiation. These progenitor cells have the unique property of self-renewal without differentiation until and unless appropriate biological and physical signals are provided. When applied to tissue engineering, for example, the use of BMPCs would offer numerous advantages, including proliferative and regenerative capability. Successful progenitor cell-based tissue engineering and regenerative medicine applications will require the cells to properly adhere to substrate. Whereas cell adhesion involves several classes of specialized proteins such as integrins, cadherins, and selectins, the cell-substrate adhesion (e.g., focal adhesion) is primarily mediated by integrins that are composed of two noncovalently bound α and β subunits (1–3). In a focal adhesion contact, integrins provide a structural function by physically linking microfilaments to the extracellular environment. Integrins not only mediate cell adhesion but also participate in the cell activation and signaling that initiate signal transduction cascades through the integrin's cytoplasmic domain (4). Further, in addition to the critical role in formation of focal adhesions, integrins have been identified to mediate cell proliferation, differentiation, migration, and apoptosis (5–7). Moreover, integrins are essential for normal development of hematopoietic lineages and bone marrow by regulating cell proliferation and differentiation (8), and the cardiomyocyte cell cycle depends on cell attachment via integrins (9).

The integrin expression level is often associated with cell differentiation. For example, neuronal differentiation involves downregulation of integrins (10) and, at successive stages of the osteoblast lineages, cells show differential patterns of integrin expression (11). Although the molecular characterization of integrin expression and pattern has been correlated with cell differentiation, it remains to be elucidated whether biophysical characterization of the integrin dynamics on the BMPC surface is dependent on the different stages of cell differentiation. For instance, because integrin diffusion to the cell-substrate contact sites is believed to regulate cell adhesion strength (12), the integrin lateral mobility on the cell surface may also correlate with cell differentiation. It appears that highly motile cells form weak focal adhesion contacts, and an inverse correlation has been established between cell adhesion and cell migration (13). Although the role of integrins involved in cell differentiation has been extensively examined (14–17), changes in the integrin diffusion characteristics at the successive stages of BMPC differentiation have not been determined.

The integrin dynamics could be determined using several biophysical techniques. For example, the fluorescence recovery after photobleaching (FRAP) technique has been used to measure the integrin lateral mobility (2,18,19). Whereas FRAP is a useful technique to measure the average integrin

Submitted August 7, 2006, and accepted for publication October 17, 2006.

Address reprint requests to Dr. Michael Cho, Dept. of Bioengineering, University of Illinois, Chicago, 851 S. Morgan St. (M/C 063), Chicago, IL 60607. Tel.: 312-413-9424; Fax: 312-996-5921; E-mail: mcho@uic.edu.

0006-3495/07/02/1399/10 $2.00

doi: 10.1529/biophysj.106.094896

dynamics over a distance of micrometer range, advanced optical techniques such as single particle tracking (SPT), which incorporates nanometer-sized gold beads, have been applied to measure the motions of individual cell surface receptors with nanometer precision (20,21). In addition, because the temporal resolution is similar, the diffusion coefficients that are two orders of magnitude smaller (e.g., microdiffusion) than those determined by FRAP can be detected (22). Using 40-nm gold beads to label integrin molecules, the role of the integrin cytoplasmic tail and its interaction with cytoskeleton has been demonstrated. For example, α_4-integrins (CD49d) were found to diffuse at the rate of 3×10^{-10} cm^2/s on the surface of Chinese hamster ovary cell but, more importantly, deletion of the α_4-integrin tail induced impaired cell adhesion and more than a threefold reduction in the diffusion coefficient (23). This finding suggests a critical role of α_4 integrins in formation of focal adhesion sites and physical attachment to cytoskeleton. Further, liganded β_1-integrins (e.g., CD29) were shown to attach to the cytoskeleton, and deletion of the β_1-integrin cytoplasmic tail prevented cytoskeletal attachment, indicating that selective ligand binding may be the critical step in regulating cell surface receptor movement and subsequent cell migration (24).

Recently, semiconductor nanocrystal quantum dots have been successfully used to track single protein dynamics (25, 26). Quantum dots have several advantages over gold beads and conventional fluorescent dyes. First, quantum dots may be used as a fluorescent probe to selectively label and monitor the nanoscale protein movement without the extensive image manipulation and analysis that are typically required of the phase-contrast gold bead images. Second, these nanocrystals are resistant to photobleaching and therefore provide much improved temporal stability (27,28). Third, unlike conventional fluorophores, only a small fraction of the receptors of interest can be labeled with functionalized quantum dots and yet provide sufficiently large signal/noise ratios to track, monitor, and identify subcellular processes in real-time. Quantum dots were also successfully used to characterize and automate cell motility and migration (29).

As reported by many authors, stem cells and BMPCs have unique structural, mechanical, and biochemical properties, which are quite different from those of fully differentiated cells (30,31). Mechanical properties such as cytoskeleton organization and elasticity, membrane tension, cell shape, and adhesion strength may play an important role in cell fate and differentiation (32) and could be correlated with integrin-dependent adhesion. In this study we used antibody-conjugated CdSe quantum dots to characterize the integrin diffusion on the surface of BMPCs at the successive stages of osteogenic differentiation at days 1, 3, 7, 10, and 14 and optically measured the cellular mechanics using laser optical tweezers (LOT). Integrins were found to diffuse slowly on the surface of undifferentiated BMPCs but, after times as early as those after a 3-day incubation in osteogenic differentiation media, integrins were able to undergo rapid lateral diffusion. The integrin lateral mobility constraints were removed by disrupting microfilaments. The LOT measurements showed that, whereas the terminally differentiated osteoblasts exhibited tightly bound cell membrane with the underlying cytoskeleton, the undifferentiated BMPC membrane was weakly associated with the cytoskeleton. These findings suggest that, together with the membrane properties, integrin lateral mobility may reflect and correlate with the state of BMPC proliferation and differentiation and that the actin-based cytoskeletal organization is largely responsible for regulation of the membrane protein dynamics in these progenitor cells.

MATERIALS AND METHODS

Cell culture

Human BMPCs were obtained from the Tulane Center for Gene Therapy (New Orleans, LA). Based on the flow cytometry results, these progenitor cells showed negative staining for CD34, CD36, CD45, and CD117 markers (all $<2\%$) and positive staining for CD44, CD90, CD166, CD29, CD49c, CD105, and CD147 markers (all $>95\%$), indicating a minimal heterogeneity in cell population. Normal human fetal osteoblasts (hFOB 1.19) were obtained from American Tissue Culture Collection (Manassas, VA). Both BMPCs and hFOB 1.19 cells were grown in Dulbecco's modified Eagle's medium containing L-glutamine, 15% fetal bovine serum, 1% penicillin/streptomycin. The cells were maintained at 37°C in 5% CO_2, harvested with trypsine/EDTA, and plated on a 22×22 mm coverslip at the initial cell seeding density of 1000 cells/cm^2. BMPCs between passages 3–9 were used for all experiments. Positive control experiments were performed to differentiate BMPCs into bone cells using the osteogenic differentiation media (10 nM dexamethasone, 20 mM β-glycerophosphate, and 50 μM L-ascorbic acid). The molecular markers such as alkaline phosphatase, calcium mineralization, and osteocalcin were used to verify the proper osteogenic differentiation. In addition, reverse transcription-polymerase chain reaction data confirmed upregulation of osteocalcins and osteopontins (data not shown).

Conjugation of quantum dots

Monoclonal antiintegrin antibodies (CD49d) were purchased from EMD Biosciences (La Jolla, CA), and CdSe quantum dots (655-nm emission wavelength) conjugated with secondary antibody were obtained from the Quantum Dot Corporation (Hayward, CA). These conjugated quantum dots were functionalized with the F(ab′)2 fragment of affinity-purified goat antibodies and cross-adsorbed against the serum proteins of numerous species. In a typical experiment, cells were blocked by 1% bovine serum albumin for 30 min and then incubated with anti-Cd49d antibodies (1:1000 dilution, final concentration 10^{-3} mg/ml) for 20 min at room temperature. Cells were washed and integrins were selectively labeled with 0.1 nM conjugated quantum dots for 20 min.

Microscopy and quantum dot motion analysis

Quantum dot movements on the cell surface were observed with a Nikon microscope (Eclipse E800) in the fluorescence and differential interference contrast (DIC) modes. An oil-immersion objective (100× PlanApo, numerical aperture (NA) = 1.4) was used to image cells and quantum dots. A filter cube was custom built to excite the CdSe quantum dots (455 ± 35 nm), and emission was detected using a 500-nm long-pass filter. The excitation

light source was a 100-W Hg lamp. For each tracking experiment, images were recorded for ~30 s at 150-ms intervals using a 16-bit charge-coupled device (CCD) camera (Photometrics, Tucson, AZ). All experiments were carried out at room temperature.

An image processor (MetaMorph, Molecular Devices, Downingtown, PA) was used to analyze the dynamics of individual quantum dots. Single nanocrystals were identified and confirmed by their blinking behavior, which is an intrinsic property of single quantum dots (33). The quantum dot position was tracked with nanometer precision using a cross correlation tracking algorithm. The cross correlation algorithm estimates the change in position of a particle by comparing an image to a kernel of a successive image. The kernel which contains the object being tracked is shifted relative to the image in one-pixel increments. For each increment, a correlation value is calculated that describes how well the values in the kernel match those of the underlying image. At the relative shift where kernel and image are most similar, a maximum in the calculated correlation matrix is found. This technique results in a subpixel displacement resolution for the tracked particles. The accuracy of position detection was determined by either tracking quantum dots immobilized on a glass surface or from analysis of quantum dot movement on fixed cells.

For each particle, mean-square displacement (MSD) for time interval $n\Delta t$ was calculated according to the formula:

$$MSD(n\Delta t) = \frac{1}{N-n-1}\sum_{i=1}^{N-n-1}\left[x(i\Delta t + n\Delta t) - x(i\Delta t)\right]^2 + \left[y(i\Delta t + n\Delta t) - y(i\Delta t)\right]^2,$$

where Δt is the time increment (i.e., 150 ms) between two successive frames, x and y are coordinates of the particle at specific times, N is the total number of frames in the sequence ($N = 200$), $0 < n < N/4$, and $1 < i < (N - 1 - n)$ are positive integers. Three modes of quantum dot-receptor conjugate motion could be distinguished from the MSD curve: simple diffusion, confined diffusion, directed diffusion modes—this can be expressed as a power law in the form of $MSD = 4D(t)t$, where the time-dependent diffusion coefficient is modified to read $D(t) = c\ t^{(\alpha-1)}$. For Brownian diffusion (i.e., $\alpha = 1$), MSD satisfies a simple relationship:

$$MSD(n\Delta t) = 4Dn\Delta t.$$

However, the microscopic diffusion coefficient D that is proportional to the slope of an MSD versus Δt plot near $\Delta t = 0$ can be determined independent of the mode of motion. Fitting a few initial data points ($n \leq 4$) of each MSD plot to a straight line yielded the microscopic diffusion coefficient D reported in this work and other previously published work (34). When the time interval is longer than $4\Delta t$ ($n > 4$), significant deviation from the straight line can be observed, for example, in the case of anomalous diffusion (e.g., restricted or directional motion).

Laser optical tweezers manipulation

Fluorescent polystyrene beads of 0.5-μm diameter (FluoSpheres, 515 nm emission, Molecular Probes, Eugene, OR) were conjugated with mouse anti-Cd29 monoclonal antibodies following standard procedure (35). The CD29 molecules are more abundantly expressed on BMPCs (36) and therefore provide a convenient molecular handle to attach and optically grab submicron beads. After incubation with cells, the membrane-attached particles were optically trapped and moved away from the cell to extract a tether from the cell membrane (see Titushkin and Cho (40) for a more detailed description). The LOT consisted of an Nd:YAG laser beam (1064 nm, 5 W maximum output power) that was focused with an oil-immersion microscope objective (100× /NA = 1.4) and translated in the specimen plane at constant speed 0.5–1.5 μm/s. Bead thermal fluctuations were measured to calibrate LOT stiffness using the equipartition theorem (37). Fluorescent images of trapped beads were recorded with a CCD camera at a 10-Hz frame rate. The tether growth was observed until the bead escaped from the trap and quickly returned to the original position. The bead position was tracked with the MetaMorph image processor, and its displacement from the trap and corresponding optical force were calculated. Typically, 35–40 beads from ~20 cells were analyzed.

RESULTS

Identification of integrin clusters and quantum dot-conjugated integrins

Confocal fluorescence microscopy was used to determine the integrin distribution on the cell surface. Using FITC-conjugated integrin antibodies, integrins (e.g., CD49d) on human osteoblasts were found to be uniformly distributed (Fig. 1 *A*). In contrast, integrin distribution on the surface of undifferentiated BMPCs was much different. First, integrins were nonuniformly expressed and found in punctates (Fig. 1 *B*). Presumably, some of the integrin clusters could represent focal contact sites that are not typically found in terminally differentiated cells (e.g., osteoblasts). Third, because the membrane protein punctates are usually associated with lateral immobility within the plane of the cell membrane, the integrin cluster formation provided a clue that the integrins on the surface of undifferentiated BMPCs may be laterally confined or restricted.

Selective integrins on the surface of BMPCs were identified and visualized using quantum dots that were conjugated with antibodies. Fig. 2 illustrates a composite of images showing the typical BMPC morphology and CdSe quantum dots conjugated with monoclonal integrin antibodies to preferentially label the $\alpha_4\beta_1$ integrin complex. The primary antibodies were diluted by 1:1000, and 0.1 nM of the quantum dot-conjugated secondary antibodies were used. This labeling protocol was sufficient and allowed us to label and identify <20 quantum dot-conjugated integrin molecules per cell. Because the cell density has been found to be a critical

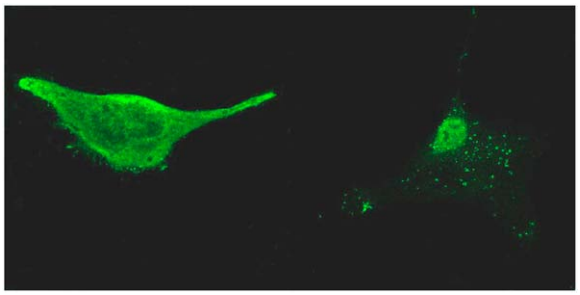

FIGURE 1 Confocal fluorescence images of integrin distribution on the surface of human osteoblast (*left panel*) and BMPC (*right panel*). Integrins were visualized using FITC-conjugated anti-CD49d antibodies. Integrins on the osteoblast were uniformly distributed. In contrast, integrins on the BMPC were found to cluster in punctates. Images were recorded using a 60×/NA = 1.4 microscope objective.

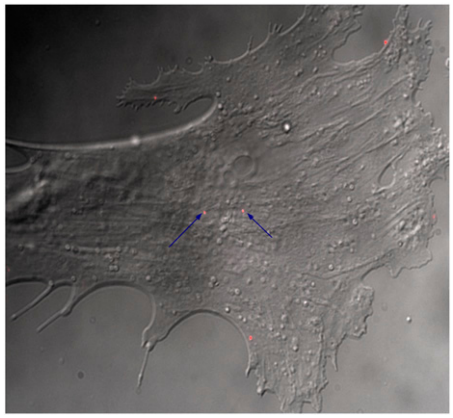

FIGURE 2 Composite overlay of DIC and fluorescence images. A typical DIC image of the BMPC was superimposed with a fluorescence image of integrins visualized using conjugated quantum dots (*red*) indicated by arrows. Optimization of antibody dilution (10^{-3} mg/ml) and quantum dot concentration (0.1 nM) resulted in labeling <20 integrin molecules per cell. Images were recorded using a 100×/NA = 1.4 microscope objective.

factor that can influence BMPC differentiation (31,32), BMPCs were plated at a low density (1000 cells/cm^2) to ensure that the intended osteogenic differentiation is optimized (32).

Measurement calibration

Quantum dot-conjugated integrin motion was monitored on the cell surface. Fig. 3, *A* and *B*, shows typical trajectories of integrin movement in osteoblasts or BMPCs at day 1, respectively. Unlike the micrometer-scale movement observed in tracking an integrin on the surface of osteoblasts (Fig. 3 *A*), the integrin movement in BMPCs was found to be severely restricted (Fig. 3 *B*). Based on these two trajectories, MSD values were computed, as described in the Materials and Methods section, and plotted as a function of time. Consistent with the trajectories, the integrin in osteoblasts was found to execute a confined movement (Fig. 3 *C*; *diamonds*) that spanned a few micrometers in the x and y axes. However, many integrin molecules observed and tracked in BMPCs were found to be laterally immobile (Fig. 3 *C*; *triangles*). In addition, the first four data points (e.g., $t < 0.6$ s) in the MSD curve were fitted to a line, and the microdiffusion coefficient was calculated from the slope of the line (34). To determine the precision of our tracking technique, cells were fixed and the integrin diffusion coefficient was measured to be $7.5 \pm 4.1 \times 10^{-12}$ cm^2/s ($n = 20$). Therefore, an integrin movement that showed a diffusion coefficient $<10^{-11}$ cm^2/s was considered laterally immobile.

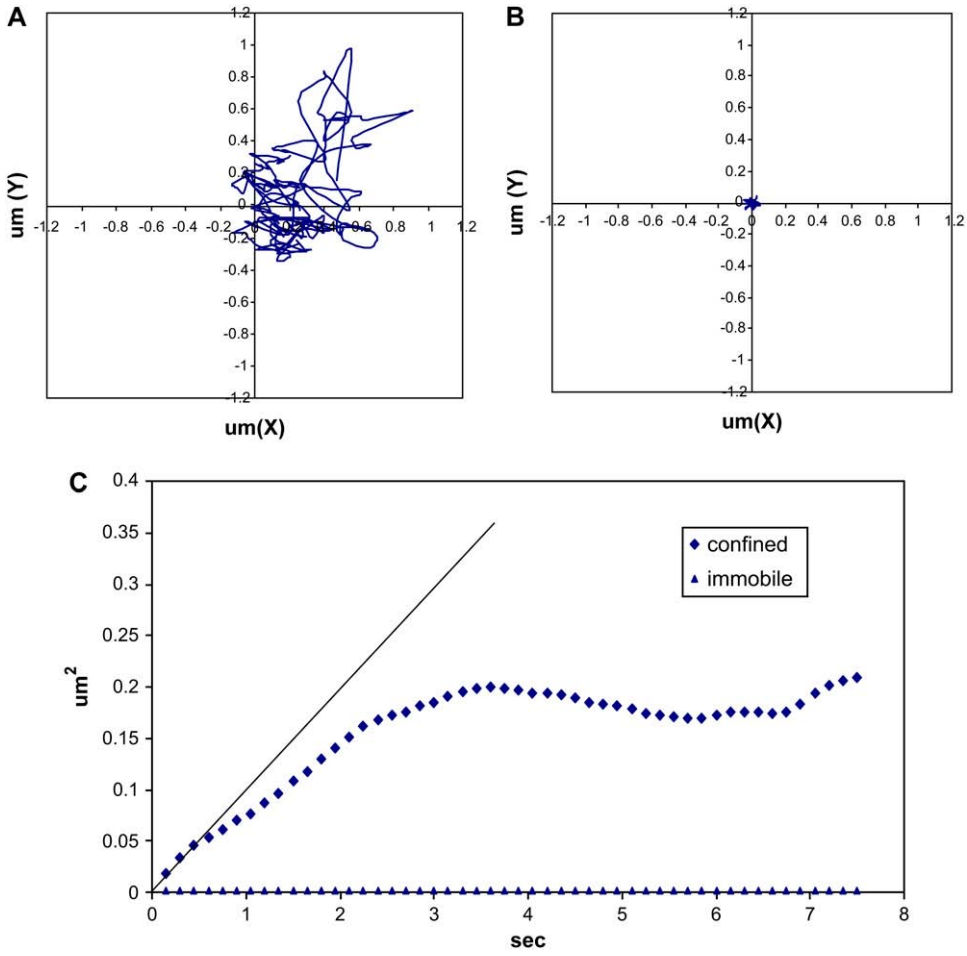

FIGURE 3 Typical integrin tracking experiment. Quantum dot-conjugated integrins were tracked for 30 s at 150-ms intervals on the cell surface. Representative trajectories of integrins monitored on the surface of human osteoblast (*A*) and BMPC (*B*) show that the integrin executed a confined movement in the terminally differentiated osteoblast (*C*, *diamonds*) but was found laterally immobile in BMPC (*C*, *triangles*). The first four data points in the integrin-confined movement were used to calculate the microdiffusion coefficient reported in this work (*solid line*).

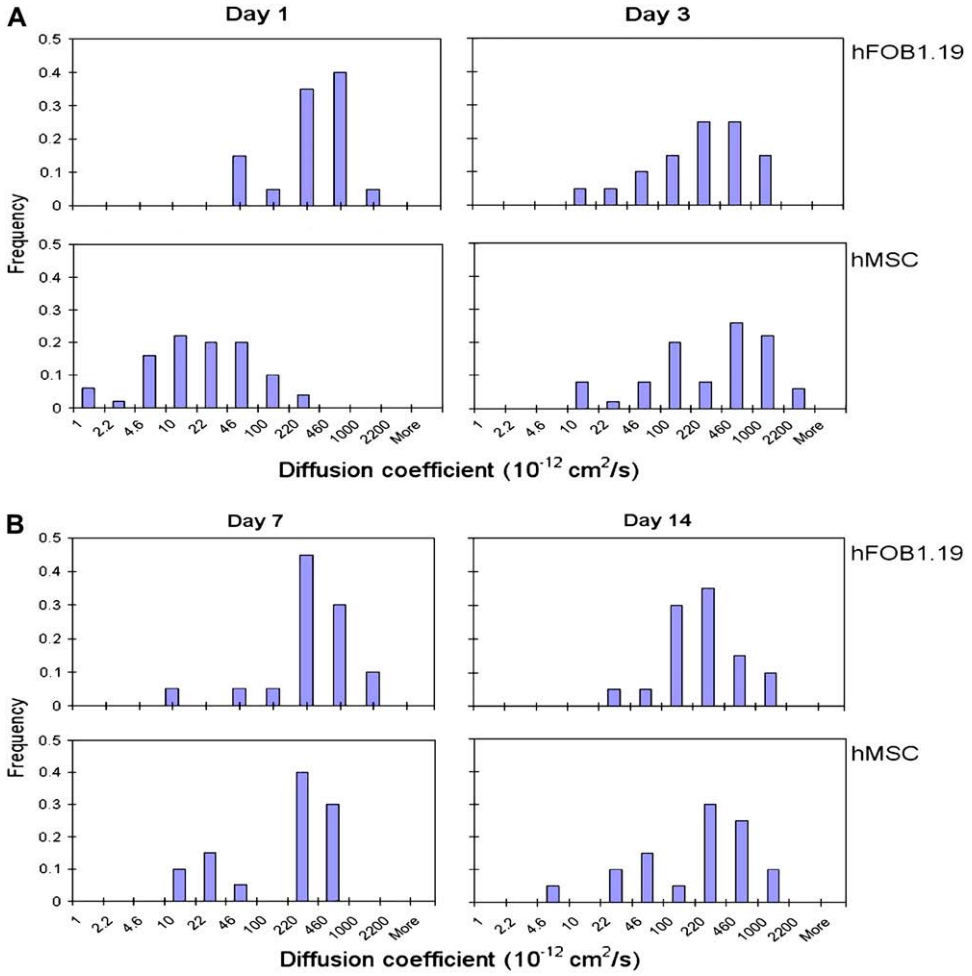

FIGURE 4 Histograms of integrin diffusion coefficients. After incubation of osteoblasts in the normal growth media for 1, 3, 7, and 14 days, the integrin diffusion coefficients were measured and histograms were constructed. To construct a histogram, at least 20 quantum dot-conjugated integrins from 3–5 osteoblasts and at least 50 integrins from 30 BMPCs were monitored, and their diffusion coefficients were determined as described in the Materials and Methods section. Histograms of integrin diffusions on human osteoblasts or BMPCs were constructed at early differentiation stages (e.g., <3 days; (*A*)) and at later stages (e.g., >7 days; (*B*)). For osteoblasts, the integrin diffusion coefficients did not statistically differ between the values determined at day 1 with those at day 3 ($p = 0.59$), day 7 ($p = 0.85$), and day 14 ($p = 0.38$). For BMPCs, the integrin diffusion coefficients became significantly greater after a 3-day incubation in the osteogenic media ($p < 0.01$) but did not further increase upon longer incubation (e.g., 7 or 14 days).

Integrin dynamics at different stages of osteogenic differentiation

To test the hypothesis that integrins undergo altered protein dynamics at later stages of BMPC osteogenic differentiation, BMPCs were incubated in the osteogenic differentiation media for 1, 3, 7, and 14 days, and the integrin diffusion was determined. For comparison, a parallel set of experiments was performed using human osteoblasts. Fig. 4 *A* shows histograms of integrin diffusion coefficients determined on the surface of terminally differentiated osteoblasts. In all four histograms constructed for integrin diffusion in human osteoblasts, no statistically significant changes were detected during the 14-day observation. Most integrins were shown to diffuse on the surface of human osteoblasts with a typical diffusion coefficient in the range of 1–5 $\times$ 10^{-10} cm^2/s. This finding is consistent with the integrin diffusion coefficient determined using conventional techniques (e.g., FRAP) (2,38). In contrast, integrins on the BMPC surface on day 1 were significantly less mobile (Fig. 4 *A*). For example, ~65% of integrins diffused with a diffusion coefficient <3 $\times$ 10^{-11} cm^2/s, suggesting that integrins at an early stage of osteogenic differentiation are confined either physically or by strong molecular interactions with cytoskeleton. Laterally restricted integrins appeared to have been freed from the mobility constraints and became increasingly mobile at the later stages of osteogenic differentiation, however. After a 3-day incubation in the osteogenic differentiation media, the diffusion coefficient histogram has shifted to the right, and >70% of integrins were found to move with a diffusion coefficient in the range of 1–5 $\times$ 10^{-10} cm^2/s (Fig. 4 *A*), which is similar to the diffusion coefficients for human osteoblasts. An additional incubation time in the osteogenic differentiation media did not further increase the integrin diffusion. After 7–14 days of osteogenic BMPC differentiation, no statistically significant increases in the integrin diffusion coefficient were observed (Fig. 4 *B*). To ensure that the osteogenic factors (e.g., dexamethasone) do not directly affect the integrin diffusion, two control experiments were performed. First, human osteoblasts were incubated in the osteogenic differentiation media for 3 days. The integrin diffusion in fully differentiated osteoblasts in the presence of the osteogenic factors was unaltered (Fig. 5 *A*). Second, BMPCs were incubated in the regular media without the osteogenic factors for 3 days. As shown in Fig. 5 *B*, integrins were found essentially immobile or diffused very slowly.

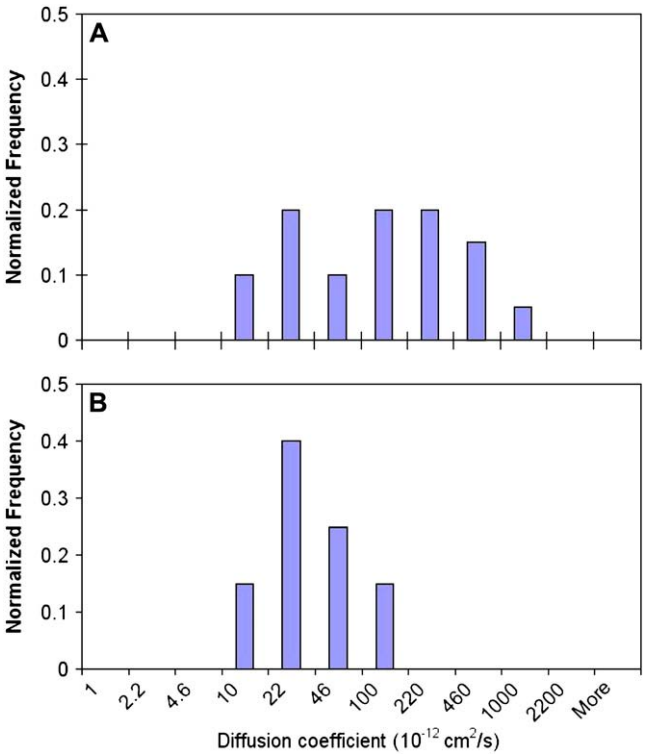

FIGURE 5 Effect of osteogenic factors on integrin diffusion. Human osteoblasts were incubated for 3 days in the osteogenic media, and the integrin diffusion coefficients were measured (*A*). Similarly, BMPCs were incubated for 3 days in the normal growth media, and the integrin diffusion coefficients were measured (*B*). These treatments did not affect or alter the integrin diffusion characteristics. The osteogenic factors do not have direct effects on the integrin diffusion. Each histogram represents data for 20–50 individual quantum dots tracked from five osteoblasts and 10 BMPCs.

These control experiments suggest that altered integrin dynamics is likely due to cellular and molecular changes in response to osteogenic differentiation but not influenced directly by the osteogenic factors.

Role of microfilaments

Actin microfilaments are one of the most important structural components of the cell cytoskeleton, which determines, to name a few, the cell shape, mobility, and mechanical properties, and membrane protein dynamics. Indeed, the compartmental model of the cell membrane (39) suggests that the microfilament structures and organization are critically involved in the membrane protein diffusion. To determine the role of microfilaments regulating integrin diffusion, cells were treated with cytochalasin D to disrupt microfilament organization. Microfilaments in human osteoblasts showed both stress fibers and a network of interconnected microfilaments (Fig. 6 *A*). In contrast, microfilaments in BMPCs were organized primarily in thicker stress fibers but lacked formation of a cytoskeletal network (Fig. 6 *B*), suggesting that the membrane-cytoskeleton association that may govern the integrin dynamics may be cell type dependent. In response to cytochalasin D treatment, the microfilament stress fibers disappeared both in human osteoblasts and BMPCs (data not shown). Integrin diffusion measurements at day 1 showed that, in response to cytochalasin D treatment, integrins were found to diffuse rapidly in human osteoblasts (Fig. 6 *C*) and also in BMPCs (Fig. 6 *D*). Therefore the microfilament disruption relaxed the integrin mobility constraints and increased the integrin diffusion. Indeed, the integrins were found to diffuse at rates ~10 times greater than that observed without cytochalasin D treatment. These findings indicate that integrin dynamics is closely associated with and regulated by microfilaments in both terminally differentiated cells and BMPCs.

Membrane-cytoskeleton association

Finally, using LOT, the membrane-cytoskeletal association was quantitatively assessed. This is rather important because, in addition to the actin-based cytoskeletal organization, the molecular association of cell cytoskeleton with the cell membrane may depend on the cell type (40) and because the membrane protein dynamics may be regulated by differential membrane mechanics. The latex beads, conjugated with antiintegrin antibodies, were optically trapped and extended to form tethers (Fig. 7). The specificity of beads binding to β_1-integrin subunits was tested with similar but not coated beads. Beads not conjugated with antibody demonstrated very low levels of binding to the cells, suggesting high binding specificity for antibody-coated probes. As shown in Fig. 8, the average length of tethers extracted from BMPC was 10.6 $\pm$ 1.1 μm, whereas osteoblasts showed a much lower average tether length (4.0 $\pm$ 1.2 μm). Our previous findings suggest that this difference is due to different membrane-cytoskeleton interactions in stem cells and fully differentiated cells (40). For example, when treated with cytochalasin D to disrupt microfilaments, the tether lengths in fully differentiated cells increased by three- to fourfold, whereas this same treatment had no effect in the tether length in BMPCs. It appears that the BMPC cytoskeleton is weakly associated with the cell membrane and that membrane mechanical properties are not altered significantly by microfilament reorganization, whereas the integrin diffusion is dictated by the physical and molecular linkage to the microfilaments.

DISCUSSION

Using SPT, we have monitored and determined the quantum dot-conjugated integrin molecules on the surface of BMPC and also terminally differentiated human osteoblasts. By optimizing the antibody concentrations, limited but selective binding and identification of integrins (e.g., ~20 integrins per cell) on the cell surface has been demonstrated. SPT analyses show that integrins on the surface of undifferentiated

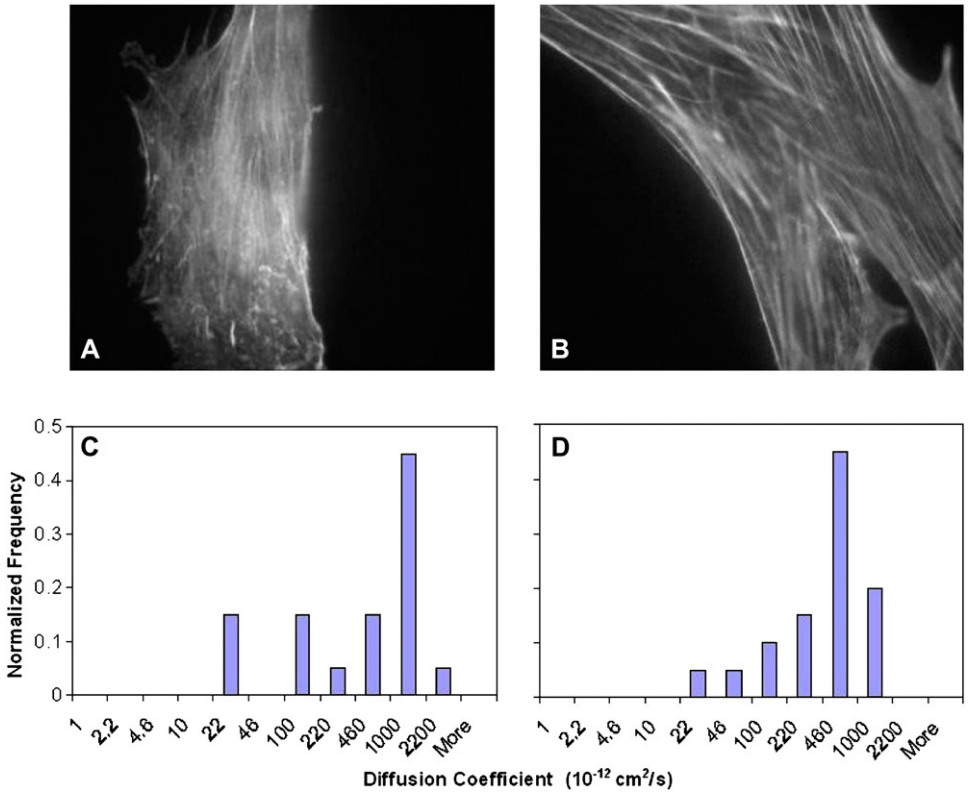

FIGURE 6 Actin cytoskeleton organization in osteoblasts (*A*) and BMPCs (*B*). BMPCs are typically bigger in size than osteoblasts and contain thicker actin stress fibers with no noticeable actin network that can be seen in osteoblasts. When microfilaments were disrupted using cytochalasin D, the integrins were found to diffuse more rapidly both in osteoblasts (*C*) and BMPCs (*D*). These two histograms of the integrin diffusion coefficients are statistically indistinguishable ($p = 0.83$). However, when compared to the control, the diffusion coefficient distributions were statistically different ($p = 0.02$ for osteoblasts and $p < 0.01$ for BMPCs). Each histogram represents data for at least 20 individual quantum dots tracked from 3–5 cells at day 1.

BMPCs either diffuse slowly or are immobile. In response to the osteogenic differentiation, integrins are observed to diffuse more rapidly at the different stages of BMPC osteogenic differentiation. For example, after a 3-day incubation in the osteogenic differentiation media, the integrin diffusion characteristics become similar to those found in the terminally differentiated human osteoblasts. Longer incubation with the osteogenic factors did not further increase the integrin diffusion, however. As anticipated, integrin dynamics in both human osteoblasts and BMPCs was regulated by the microfilament organization. Based on the LOT experiments, the BMPC membrane was found to be weakly coupled with actin cytoskeleton, suggesting that the membrane protein dynamics is regulated largely by the cytoskeletal organization, and the cellular mechanics plays a minor role. Collectively, these findings indicate that the integrin lateral mobility on the surface of undifferentiated BMPC is severely constrained by microfilaments that appear to relax at later stages of BMPC differentiation and therefore may be correlated with BMPC differentiation.

Unlike conventional techniques (e.g., FRAP) that were developed to measure the molecule movement over a micrometer scale, SPT is capable of determining the microscopic diffusion coefficients of the membrane molecules. Based on SPT experiments using the quantum dots conjugated with integrin antibodies, integrins in the human osteoblast membrane show the typical diffusion coefficients in the range of 10^{-9}–10^{-10} cm^2/s (Fig. 4 *A*). The characteristic distance traversed by an integrin molecule during a 0.6-s measurement time period (i.e., the first four data points in the MSD curve) would be ~340 nm (assuming $D = 5 \times 10^{-10}$ cm^2/s). This value is less than the typical domain size, which has been determined to be ~500 nm (34), suggesting that an integrin molecule is unlikely to hop from one domain over to the next domain during this time of observation. Therefore, the measurements of integrin diffusion coefficient in this study can be considered to represent the microscopic integrin dynamics. Extending the integrin movement trajectories over 10 s, random and confined movements can be distinguished based on the MSD analysis. For example, the random movement would correlate with a linear increase in MSD, whereas

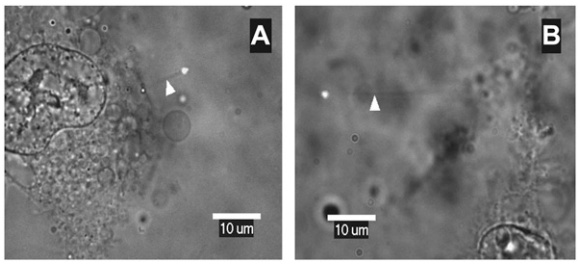

FIGURE 7 Membrane tethers extracted from osteoblasts (*A*) and BMPCs (*B*). Fluorescent beads (0.5-μm diameter) were attached to the cell membrane and pulled away from the cell by LOT. The thin membrane tethers extending from the beads to the cell body (*white arrows*) appear as faint shadows in the superimposed brightfield/fluorescence images.

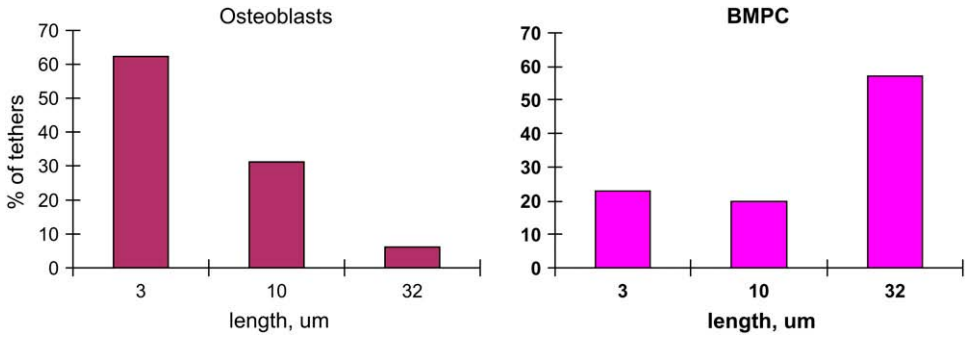

FIGURE 8 Tether extraction experiment. The motion of the laser tweezers with the trapped bead continued at constant speed 1.5 μm/s until the bead escaped and quickly retracted to the cell surface. The tether length was determined from images recorded at 0.1-s intervals. At day 1, the tether lengths in osteoblasts and BMPCs were determined. The optical forces applied to produce these tethers were estimated to be between 3 and 10 pN. The tether length distributions, constructed from measurements of 35–40 tethers (n = 20–25 cells), show that longer tethers could be produced more frequently in undifferentiated BMPCs, indicating a weaker cell membrane-cytoskeleton association.

the confined movement would cause the MSD curve to saturate (see Fig. 3). At day 1, ~55% and 95% of integrins monitored in the membrane of osteoblasts and BMPCs showed the confined movement, respectively. After a 3-day incubation in the osteogenic media, 65% of integrins in the BMPC membrane were quantified to execute the confined movement. Therefore, in addition to achieving the typical diffusion coefficient in the membrane of BMPCs, the fraction of integrins freed from the lateral mobility constraints and able to diffuse also became comparable to that found in the terminally differentiated osteoblasts.

In intact cell membranes, integrins are known to diffuse at rates on the order of 10^{-9} to 10^{-10} cm^2/s (41,42), whereas lipids or lipid-linked proteins diffuse at faster rates (10^{-8} to10^{-9} cm^2/s) (38,43), suggesting that the typical membrane proteins are confined or constrained by molecular interactions. At least three mechanisms could be involved to restrict the integrin mobility constraints on the BMPC surface. First, integrins may be clustered, thus unable to diffuse in the cell membrane. Fluorescent images recorded using fluorescently conjugated integrin antibodies (Fig. 1) show that the initial distribution of integrins on the BMPC surface at day 1 is nonuniform and localized in visible integrin punctates, indicating that integrin clusters are likely present. Receptor clustering alone, however, may not bear significant effects on the receptor diffusion (44). Second, based on the findings that integrins are essentially immobile, integrins could interact directly with the cytoskeleton. This postulate is supported by the findings that treatment of BMPCs with cytochalasin D causes integrins to diffuse more rapidly (Fig. 6). Third, the membrane protein mobility constraints can be adequately explained by a model in which the cell membrane is compartmentalized by the cytoskeletal organization (45). This is sometimes referred to as the fence model, where the receptor diffusion is restricted within the membrane domains determined by underlying cytoskeleton (34). Inside these domains, molecules move with microscopic diffusion coefficient around 5×10^{-10} cm^2/s. However, whereas the microfilament organization in human osteoblasts appears to be compartmentalized (see Fig. 6 *A*), the similar cytoskeletal arrangement is not clearly observed in BMPCs. For example, the microfilaments in BMPCs (Fig. 6 *B*) exhibit thicker stress fibers and the lack of an interconnected network, which would suggest the BMPC cytoskeletal organization in the undifferentiated state differs from that observed after differentiation. This observation is consistent with recently reported findings (30) that BMPCs undergo considerable morphological and microfilament reorganization as these cells differentiate. Rather than sterically confined in the microfilament-based membrane compartments (e.g., fence model), the restricted integrin's lateral mobility in BMPCs appears to be unique to undifferentiated progenitor cells and is likely due to physical integrin-microfilament attachments. These molecular constraints are likely responsible for laterally much less mobile integrins in the undifferentiated BMPC membrane. However, we cannot completely rule out the possibility that our observations could, in part, be attributed to the heterogeneity of the BMPC populations.

Furthermore, in terminally committed cells (e.g., osteoblasts or fibroblasts), the plasma membrane may be strongly associated with the underling meshwork of thin actin fibers through multiple weak links such as lipid-protein bonds (40). Because the membrane receptor diffusion is regulated by steric hindrance imposed by the underlying cytoskeletal structure, integrins can diffuse rapidly within the membrane domains formed by the actin meshwork and diffuse across from one domain to anther. In contrast, in progenitor cells, thick actin stress fibers are connected with the membrane only at a few discrete sites (e.g., focal adhesions). Weaker but multiple attachments of intracellular structural proteins to the lipid bilayer surface in osteoblasts could result in a stronger membrane-cytoskeleton adhesion in comparison with stronger but fewer contacts between the membrane and cytoskeleton in the progenitor cells. A minimal effect of cytoskeleton disintegration on the membrane tether length suggests a much weaker membrane-cytoskeleton association in BMPCs. In agreement with SPT results, the integrin clusters that may be directly linked to the microfilaments

would be laterally immobile despite a weaker membrane-cytoskeletal attachment.

Finally, osteogenic differentiation is typically verified by using numerous cellular and molecular markers such as alkaline phosphotase, calcium mineralization, and osteocalcin. Some of these markers do not appear until ~10 days after osteogenic differentiation, however (46,47). A 3-day incubation of BMPCs with the osteogenic factors is perhaps too premature to be categorized as specific osteogenic differentiation. This observation may be important because relaxation of integrin mobility constraints may be correlated with but not sufficient to induce BMPC differentiation into specific tissue lineages. This postulate is supported by the results that integrins remain laterally immobile in BMPCs when the cells were not treated with the osteogenic factors and that the osteogenic factors do not affect the integrin dynamics in terminally differentiated osteoblasts (Fig. 5). Rather, it appears that laterally mobile integrins are one of the early biophysical events that are involved in BMPC proliferation and differentiation. However, it remains to be determined whether relaxation of the membrane protein lateral mobility is specific to the osteogenic differentiation or whether removal of such biophysical constraints may be applicable to BMPC differentiation into other tissue lineages.

SUMMARY

The combined use of quantum dot-conjugated molecules and SPT is a powerful biophysical technique to elucidate the physical constraints on the protein mobility at the cell surface. Our findings show that there is a major shift in the integrin mobility from the undifferentiated BMPC membrane to different stages of BMPC differentiation. Unlike the typical integrin diffusion found at the later stages of osteogenic differentiation, the integrins in undifferentiated BMPCs are found to diffuse slowly. After a 3-day differentiation, the integrin diffusion became no longer distinguishable from that measured on the terminally differentiated human osteoblasts. Future studies of other protein mobility in undifferentiated BMPCs may serve to extend these observations to other classes of membrane proteins that, like integrins, are severely constrained by the cytoskeleton (i.e., microfilaments) yet able to diffuse rapidly in the plane of the membrane under conditions of cytoskeletal reorganization that could accompany cell differentiation. Finally, when the membrane mechanical properties of BMPCs were studied with the LOTs technique, much longer tethers were extracted from the BMPC plasma membrane than those from fully differentiated osteoblasts, suggesting that differential integrin dynamics may be attributed to the different membrane mechanics. In human osteoblasts, the membrane is tightly bound to the cytoskeleton, and integrins are confined in the domains that are defined by the microfilament network. In progenitor cells, however, the distinctive and unusual mechanical properties of the cell membrane can be attributed to its weak attachment to the cytoskeleton (e.g., actins), and slow integrin diffusion or lateral immobilization are likely due to direct association of integrins with microfilaments.

This work was supported, in part, by National Institutes of Health grants (GM060741, EB006067) and a grant from the Office of Naval Research (N00014-06-1-0100).

REFERENCES

1. Cox, E. A., and A. Huttenlocher. 1998. Regulation of integrin-mediated adhesion during cell migration. *Microsc. Res. Tech.* 43: 412–419.
2. Webb, D. J., C. M. Brown, and A. F. Horwitz. 2003. Illuminating adhesion complexes in migrating cells: moving toward a bright future. *Curr. Opin. Cell Biol.* 15:614–620.
3. Arnaout, M. A., B. Mahalingam, and J. P. Xiong. 2005. Integrin structure, allostery, and bidirectional signaling. *Annu. Rev. Cell Dev. Biol.* 21:381–410.
4. Juliano, R. L. 2002. Signal transduction by cell adhesion receptors and the cytoskeleton: functions of integrins, cadherins, selectins, and immunoglobulin-superfamily members. *Annu. Rev. Pharmacol. Toxicol.* 42:283–323.
5. Hynes, R. O. 1992. Integrins: versatility, modulation, and signaling in cell adhesion. *Cell.* 69:11–25.
6. Schwartz, M. A., M. D. Schaller, and M. H. Ginsberg. 1995. Integrins: emerging paradigms of signal transduction. *Annu. Rev. Cell Dev. Biol.* 11:549–599.
7. Tate, M. C., A. J. Garcia, B. G. Keselowsky, M. A. Schumm, D. R. Archer, and M. C. LaPlaca. 2004. Specific β_1 integrins mediate adhesion, migration, and differentiation of neural progenitors derived from the embryonic striatum. *Mol. Cell Neurosci.* 27:22–31.
8. Arroyo, A. G., J. Y. Yang, H. Rayburn, and R. O. Hynes. 1999. α_4 integrins regulate the proliferation/differentiation balance of multilineage hematopoietic progenitors in vivo. *Immunity.* 11:555–566.
9. Maitra, N., I. L. Flink, J. Bahl, and E. Morkin. 2000. Expression of α and β integrins during terminal differentiation of cardiomyocytes. *Cardiovasc. Res.* 47:715–725.
10. Yoshida, N., S. Hishiyama, M. Yamaguchi, M. Hashiguchi, Y. Miyamoto, S. Kaminogawa, and T. Hisatsune. 2003. Decrease in expression of $\alpha_5\beta_1$ integrin during neuronal differentiation of cortical progenitor cells. *Exp. Cell Res.* 287:262–271.
11. Bennett, J. H., D. H. Carter, A. L. Alavi, J. N. Beresford, and D. Walsh. 2001. Patterns of integrin expression in a human mandibular explant model of osteoblast differentiation. *Arch. Oral Biol.* 46:229–238.
12. Novak, I. L., B. M. Slepchenko, A. Mogilner, and L. M. Loew. 2004. Cooperativity between cell contractility and adhesion. *Phys. Rev. Lett.* 93:268109.
13. Ridley, A. J., M. A. Schwartz, K. Burridge, R. A. Firtel, M. H. Ginsberg, G. Borisy, J. T. Parsons, and A. R. Horwitz. 2003. Cell migration: integrating signals from front to back. *Science.* 302:1704–1709.
14. Giancotti, F. G., and E. Ruoslahti. 1999. Integrin signaling. *Science.* 285:1028–1033.
15. Wijelath, E. S., S. Rahman, J. Murray, Y. Patel, G. Savidge, and M. Sobel. 2004. Fibronectin promotes VEGF-induced CD34 cell differentiation into endothelial cells. *J. Vasc. Surg.* 39:655–660.
16. Watt, F. M. 2002. Role of integrins in regulating epidermal adhesion, growth and differentiation. *EMBO J.* 21:3919–3926.
17. Foster, L. J., P. A. Zeemann, C. Li, M, Mann, O. N. Jensen, and M. Kassem. 2005. Differential expression profiling of membrane proteins by quantitative proteomics in a human mesenchymal stem cell line undergoing osteoblast differentiation. *Stem Cells.* 23:1367–1377.
18. Johnson, M. E., D. A. Berk, D. Blankschtein, D. E. Golan, R. K. Jain, and R. S. Langer. 1996. Lateral diffusion of small compounds in

human stratum corneum and model lipid bilayer systems. *Biophys. J.* 71:2656–2668.

19. Tang, Q., and M. Edidin. 2003. Lowering the barriers to random walks on the cell surface. *Biophys. J.* 84:400–407.
20. Saxton, M. J., and K. Jacobson. 1997. Single-particle tracking: applications to membrane dynamics. *Annu. Rev. Biophys. Biomol. Struct.* 26:373–399.
21. Murase, K, T. Fujiwara, Y. Umemura, K. Suzuki, R. Iino, H. Yamashita, M. Saito, H. Murakoshi, K. Ritchie, and A. Kusumi. 2004. Ultrafine membrane compartments for molecular diffusion as revealed by single molecule techniques. *Biophys. J.* 86:4075–4093.
22. Mirchev, R., and D. E. Golan. 2001. Single-particle tracking and laser optical tweezers studies of the dynamics of individual protein molecules in membranes of intact human and mouse red cells. *Blood Cells Mol. Dis.* 27:143–147.
23. Yauch, R. L., D. P. Felsenfeld, S. K. Kraeft, L. B. Chen, M. P. Sheetz, and M. E. Hemler. 1997. Mutational evidence for control of cell adhesion through integrin diffusion/clustering, independent of ligand binding. *J. Exp. Med.* 186:1347–1355.
24. Felsenfeld, D. P., D. Choquet, and M. P. Sheetz. 1996. Ligand binding regulates the directed movement of β_1 integrins on fibroblasts. *Nature.* 383:390–391.
25. Dahan, M., S. Levi, C. Luccardini, P. Rostaing, B. Riveau, and A. Triller. 2003. Diffusion dynamics of glycine receptors revealed by single-quantum dot tracking. *Science.* 302:442–445.
26. Alexson, D., H. Chen, M. R. Cho, M. Dutta, Y. Li, P. Shi, A. Raichura, D. Ramadurai, S. Parikh, M. Stroscio, and M. Vasudev. 2005. Semiconductor nanostructures in biological applications. *J. Phys. Condens. Matter.* 17:R637–R656
27. Lidke, D. S., P. Nagy, R. Heintzmann, D. J. Arndt-Jovin, J. N. Post, H. E. Grecco, E. A. Jares-Erijman, and T. M. Jovin. 2004. Quantum dot ligands provide new insights into erbB/HER receptor-mediated signal transduction. *Nat. Biotechnol.* 22:198–203.
28. Jaiswal, J. K., H. Mattoussi, J. M. Mauro, and S. M. Simon. 2003. Long-term multiple color imaging of live cells using quantum dot bioconjugates. *Nat. Biotechnol.* 21:47–51.
29. Pellegrino, T., W. J. Parak, R. Boudreau, M. A. Le Gros, D. Gerion, A. P. Alivisatos, and C. A. Larabell. 2003. Quantum dot-based cell motility assay. *Differentiation.* 71:542–548.
30. Rodriguez, J. P., M. Gonzalez, S. Rios, and V. Cambiazo. 2004. Cytoskeletal organization of human mesenchymal stem cells (MSC) changes during their osteogenic differentiation. *J. Cell Biochem.* 93: 721–731.
31. Pittenger, M. F., A. M. Mackay, S. C. Beck, R. K. Jaiswal, R. Douglas, J. D. Mosca, M. A. Moorman, D. W. Simonetti, S. Craig, and D. R. Marshak. 1999. Multilineage potential of adult human mesenchymal stem cells. *Science.* 284:143–147.
32. McBeath, R., D. M. Pirone, C. M. Nelson, K. Bhadriraju, and C. S. Chen. 2004. Cell shape, cytoskeletal tension, and RhoA regulate stem cell lineage commitment. *Dev. Cell.* 6:483–495.
33. Nirmal, M., B. O. Dabbousi, M. G. Bawendi, J. J. Macklin, J. K. Trautman, T. D. Harris, and L. E. Brus. 1996. Fluorescence intermittency in single cadmium selenide nanocrystals. *Nature.* 38:802–804.
34. Kusumi, A., Y. Sako, and M. Yamamoto. 1993. Confined lateral diffusion of membrane receptors as studied by single particle tracking (nanovid microscopy). Effects of calcium-induced differentiation in cultured epithelial cells. *Biophys. J.* 65:2021–2040.
35. Fallman, E., S. Schedin, J. Jass, M. Andersson, B. E. Uhlin, and O. Axner. 2004. Optical tweezers based force measurement system for quantitating binding interactions: system design and application for the study of bacterial adhesion. *Biosens. Bioelectron.* 19:1429–1437.
36. Grayson, W. L., T. Ma, and B. Bunnell. 2004. Human mesenchymal stem cells tissue development in 3D PET matrices. *Biotechnol. Prog.* 20:905–912.
37. Neuman, K. C., and S. M. Block. 2004. Optical trapping. *Rev. Sci. Instrum.* 75:2787–2809.
38. Wehrle-Haller, B., and B. Imhof. 2002. The inner lives of focal adhesions. *Trends Cell Biol.* 12:382–389.
39. Sako, Y., and A. Kusumi. 1994. Compartmentalized structure of the plasma membrane for receptor movements as revealed by a nanometer-level motion analysis. *J. Cell Biol.* 125:1251–1264.
40. Titushkin, I., and M. Cho. 2006. Distinct membrane mechanical properties of human mesenchymal stem cell determined using laser optical tweezers. *Biophys. J.* 90:2582–2591.
41. Schootemeijer, A., G. van Willigen, H. van der Vuurst, L. G. Tertoolen, S. W. De Laat, and J. W. Akkerman. 1997. Lateral mobility of integrin alpha IIb beta 3 (glycoprotein IIb/IIIa) in the plasma membrane of a human megakaryocyte. *Thromb. Haemost.* 77:143–149.
42. Hirata, H., K. Ohki, and H. Miyata. 2005. Mobility of integrin alpha5beta1 measured on the isolated ventral membranes of human skin fibroblasts. *Biochim. Biophys. Acta.* 1723:100–105.
43. Cho, M. R., D. W. Knowles, B. L. Smith, J. J. Moulds, P. Agre, N. Mohandas, and D. E. Golan. 1999. Membrane dynamics of the water transport protein AQP1 in intact human red blood cells. *Biophys. J.* 76:1136–1144.
44. Saffman, P. G., and M. Delbruck. 1975. Brownian motion in biological membrane. *Proc. Natl. Acad. Sci. USA.* 72:3111–3113.
45. Sako, Y., and A. Kusumi. 1995. Barriers for lateral diffusion of transferrin receptor in the plasma membrane as characterized by receptor dragging by laser tweezers: fence versus tether. *J. Cell Biol.* 129:1559–1574.
46. Payne, R. G., M. J. Yaszemski, A. W. Yasko, and A. G. Mikos. 2002. Development of an injectable, in situ crosslinkable, degradable polymeric carrier for osteogenic cell populations. Part 1. Encapsulation of marrow stromal osteoblasts in surface crosslinked gelatin microparticles. *Biomaterials.* 23:4359–4371.
47. Meinel, L., V. Karageorgiou, R. Fajardo, B. Snyder, V. Shinde-Patil, L. Zichner, D. Kaplan, R. Langer, and G. Vunjak-Novakovic. 2004. Bone tissue engineering using human mesenchymal stem cells: effects of scaffold material and medium flow. *Ann. Biomed. Eng.* 32:112–122.